ChemPubSoc Europe

DOI: 10.1002/cbic.201600285

CHEMBIOCHEM Full Papers

Galectin-3-Binding Glycomimetics that Strongly Reduce Bleomycin-Induced Lung Fibrosis and Modulate Intracellular Glycan Recognition

Tamara Delaine,[a] Patrick Collins,[b] Alison MacKinnon,[c] G. Sharma ,[d] John Stegmayr,[d] Vishal K. Rajput,[a] Santanu Mandal,[a] Ian Cumpstey,[a] Amaia Larumbe,[a] Bader A. Salameh,[a, i] Barbro Kahl-Knutsson,[d] Hilde van Hattum,[e] Monique van Scherpenzeel,[e, j] Roland J. Pieters,[e] Tariq Sethi,[f] Hans Schambye,[g] Stina Oredsson,[h] Hakon Leffler,[d] Helen Blanchard,*[b] and Ulf J. Nilsson*[a]

Discovery of glycan-competitive galectin-3-binding compounds that attenuate lung fibrosis in a murine model and that block intracellular galectin-3 accumulation at damaged vesicles, hence revealing galectin-3–glycan interactions involved in fibrosis progression and in intracellular galectin-3 activities, is reported. 3,3′-Bis-(4-aryltriazol-1-yl)thiodigalactosides were synthesized and evaluated as antagonists of galectin-1, -2, -3, and -4 N-terminal, -4 C-terminal, -7 and -8 N-terminal, -9 N-terminal, and -9 C-terminal domains. Compounds displaying low-nanomolar affinities for galectins-1 and -3 were identified in a competitive fluorescence anisotropy assay. X-ray structural analysis of selected compounds in complex with galectin-3, together with galectin-3 mutant binding experiments, revealed that both the aryltriazolyl moieties and fluoro substituents on the compounds are involved in key interactions responsible for exceptional affinities towards galectin-3. The most potent galectin-3 antagonist was demonstrated to act in an assay monitoring galectin-3 accumulation upon amitriptyline-induced vesicle damage, visualizing a biochemically/medically relevant intracellular lectin–carbohydrate binding event and that it can be blocked by a small molecule. The same antagonist administered intratracheally attenuated bleomycin-induced pulmonary fibrosis in a mouse model with a dose/response profile comparing favorably with that of oral administration of the marketed antifibrotic compound pirfenidone.

Introduction

The galectins are a family of proteins that have the ability to crosslink β-D-galactopyranoside-containing glycoproteins (and other glycoconjugates) to form lattices[1] and thereby modulate glycoprotein localization, transport, and residence times in cellular compartments and at surfaces.[2] Crosslinking of glycoproteins through the action of galectins can occur due to the galectins' capability to present multiple carbohydrate recognition domains (CRDs) depending on their type. Prototypical galectins (-1, -2, -5, -7, -10, -11, -13, -14, and -15) each contain one CRD but dimerize depending on their concentration and

[a] Dr. T. Delaine, Dr. V. K. Rajput, Dr. S. Mandal, Dr. I. Cumpstey, Dr. A. Larumbe, Dr. B. A. Salameh, Prof. U. J. Nilsson
Centre for Analysis and Synthesis
Department of Chemistry, Lund University
P.O. Box 124, 221 00 Lund (Sweden)
E-mail: ulf.nilsson@chem.lu.se

[b] Dr. P. Collins, Assoc. Prof. H. Blanchard
Institute for Glycomics, Griffith University
Gold Coast Campus, Queensland 4222 (Australia)
E-mail: h.blanchard@griffith.edu.au

[c] Dr. A. MacKinnon
MRC Centre for Inflammation Research
The Queen's Medical Research Institute, University of Edinburgh
49 Little France Crescent, Edinburgh EH16 4TJ (UK)

[d] Dr. G. Sharma , J. Stegmayr, B. Kahl-Knutsson, Prof. H. Leffler
Department of Laboratory Medicine, Section MIG, Lund University
BMC-C1228b, Klinikgatan 28, 221 84 Lund (Sweden)

[e] Dr. H. van Hattum, Dr. M. van Scherpenzeel, Prof. R. J. Pieters
Department of Medicinal Chemistry and Chemical Biology
Utrecht Institute for Pharmaceutical Sciences, Utrecht University
P.O. Box 80082, 3508 TB Utrecht (Netherlands)

[f] Prof. T. Sethi
Department of Respiratory Medicine and Allergy, Kings College
41 Denmark Hill Campus, Bessemer Road, London SE5 9RJ (UK)

[g] Dr. H. Schambye
Galecto Biotech ApS, COBIS
Ole Maaloes vej 3, Copenhagen N 2200 (Denmark)

[h] Prof. S. Oredsson
Department of Biology, Lund University
P.O. Box 118, 221 00 Lund (Sweden)

[i] Dr. B. A. Salameh
Present address: Chemistry Department, The Hashemite University
P.O. Box 150459, Zarka 13115 (Jordan)

[j] Dr. M. van Scherpenzeel
Present address: Translational Metabolic Laboratory
51 Radboud University Medical Center
P.O. Box 9101, 6500 HB Nijmegen (Netherlands)

Supporting information for this article can be found under http://dx.doi.org/10.1002/cbic.201600285.

ligand density. The tandem-repeat galectins (-4, -6, -8, -9, and -12) each contain and present two CRDs, and the chimera-type galectin-3 CRD is linked to a glycine/proline-rich collagen-like N-terminal domain that enables oligomerization.

This organizational lattice-forming role of the galectins influences glycoprotein activities and their duration, as well as glycoprotein intracellular trafficking and sorting. This manifests itself in different effects at the cellular level that depend on a match between galectin type and expression, as well as on the glycan structures in the cell. For example, galectin–glycoconjugate interactions control cell properties and functions and cell adhesion, as well as having immunomodulatory effects[3] and effects on tumor growth and metastases.[4] The cellular mechanisms and roles in inflammation and cancer point to the use of galectin CRD antagonists as therapeutic agents, and several ex vivo[5] and in vivo[6] studies of the most intensely studied and best-characterized galectin-3 have corroborated such hypotheses.

Among attempts to develop small-molecule and drug-like compounds as galectin-3 antagonists, substitution of galactose[6a,7] [either as such or as part of lactose or *N*-acetyllactosamine (LacNAc)] and 3,3-disubstitution of thiodigalactoside[8] have proven to be successful. In particular, high-affinity small-molecule galectin-3 antagonists with sub-micromolar affinities have been discovered by appending aromatic amido groups or 4-amido-1,2,3-triazolyl groups at both C3 carbon atoms in thiodigalactoside.[8a,b,d] Here we present (4-aryl-1,2,3-triazolyl)thiodigalactoside-based derivatives as significantly improved antagonists with selectivity for galectins-1 and -3. Furthermore, an investigation based on three X-ray structures of galectin-3 in complex with inhibitors and on galectin-3 mutant studies revealed that the aryltriazolyl groups form affinity-enhancing interactions with arginine side chains and with β-strand backbones. One selected compound was demonstrated to function intracellularly in an amitriptyline-induced vesicle damage assay and to reduce fibrosis levels in a murine bleomycin lung fibrosis model.

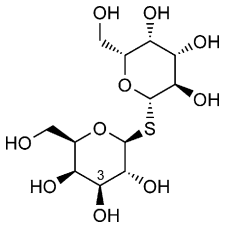

Results and Discussion

Synthesis

The ditriazolylthiodigalactosides **3**–**10** and **12** were synthesized by Cu^{I}-catalyzed cycloadditions between the known diazide **1**[9] and phenylacetylenes (Scheme 1). The syntheses of the unsubstituted phenyltriazole **2** and the phenoxyphenyltriazole **11** have been reported previously.[10] The 1-naphthyltriazole **7** was synthesized essentially by following a previously published alternative procedure[8d] that involved cycloaddition between 1-ethynylnaphthalene and the azidogalactose derivative **13**[11] to give the triazole **14**. Bromination of **14** and subsequent double substitution of the bromide **15** with sodium sulfide resulted in

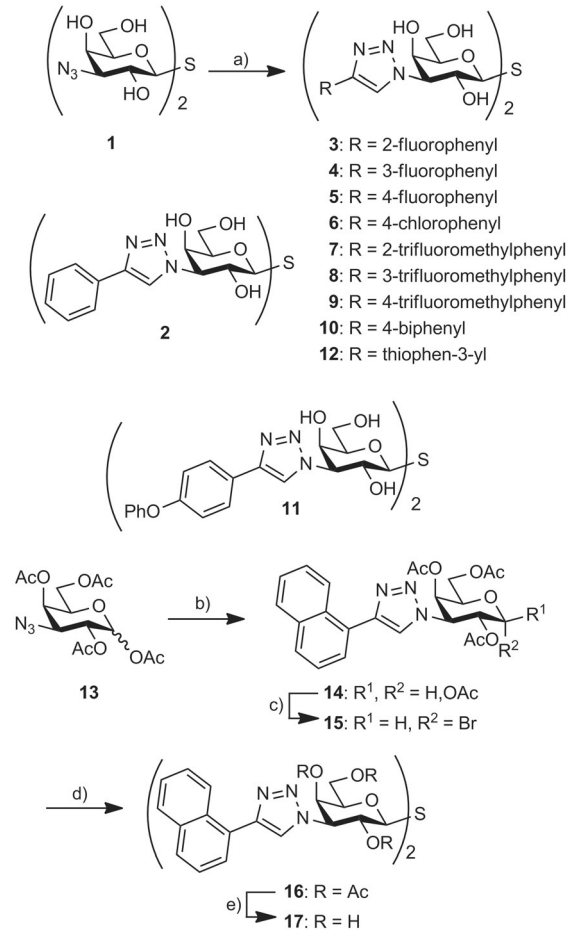

Scheme 1. a) Alkyne, CuI, Et_3N, DMF; b) alkyne, CuI, DIPEA, toluene, 65–80 °C; c) HBr/AcOH; d) Na_2S, MS 4 Å, MeCN; e) $BuNH_2$, MeOH.

the thiodigalactoside **16** in a moderate yield. De-*O*-acetylation of **16** gave the target 1-naphthyltriazole **17**.

Galectin affinities and structure–activity relationships

With a panel of bis(aryltriazolyl)thiodigalactosides **2**–**12** and **17** to hand, affinities towards galectin-1, -2, -3 and -4 N- and C-terminal domains, -7 and 8 N-terminal domain, and -9 N- and C-terminal domains were determined in a competitive protein-binding assay based on fluorescence anisotropy as described in detail previously.[12] Except for galectin-8N, all investigated galectins bound all, or most, of the inhibitors **2**–**12** and **17** with affinities significantly greater than those of the parent unsubstituted thiodigalactoside (Table 1). Galectin-1 indeed bound all unsubstituted phenyltriazoles or those with smaller substituents (**2**–**9**) with high affinities, whereas the presence of larger substituents (**10** and **11**) significantly reduced affinity. Interestingly, 3- and 4-fluorophenyl compounds **4** and **5** turned out to be the only ones better than the unsubstituted phenyl compound **2** and the 2-fluorophenyl derivative **3**, with dissociation constants as low as 12 nM (3-fluorophenyl derivative **4**).

This suggests that one or both of the galectin-1 subsites that accommodate the phenyl groups of **2**–**11** are tight with limited possibilities for substitutions, as also suggested on the

Table 1. Dissociation constants for **2**–**12**, **17**, and galectin-1, -2, -3, -4, -4N-terminal domain, -4C-terminal domain, -7, -8N-terminal domain, and -9N- and -9C-terminal domain determined by competitive fluorescence anisotropy assay.[12]

Galectin	Dissociation constant [μM]								
	-1	-2	-3	-4N	-4C	-7	-8N	-9N	-9C
2	0.049[10]	1.2 ± 0.27	0.044[10]	2.6 ± 0.25	0.19 ± 0.015	1.2 ± 0.21	> 100	2.3 ± 0.23	0.98 ± 0.16
3	0.31 ± 0.045	0.98 ± 0.12	0.19 ± 0.033	2.9 ± 0.63	0.39 ± 0.083	1.6 ± 0.17	83 ± 9.9	1.0 ± 0.28	1.4 ± 0.22
4	0.012 ± 0.003	> 5	0.014 ± 0.003	0.17 ± 0.029	0.14 ± 0.042	1.9 ± 0.38	86 ± 8.8	0.68 ± 0.34	0.12 ± 0.015
5	0.027 ± 0.003	> 5	0.034 ± 0.0058	0.65 ± 0.24	0.073 ± 0.003	4.2 ± 0.79	104 ± 15	1.8 ± 0.20	0.58 ± 0.10
6	0.33 ± 0.030	10 ± 3.9	0.19 ± 0.044	7.2 ± 1.2	4.7 ± 0.34	3.4 ± 0.56	210 ± 19	2.8 ± 0.76	1.8 ± 0.36
7	1.4 ± 0.70	1.5 ± 0.44	0.38 ± 0.039	3.8 ± 0.35	4.9 ± 0.87	2.0 ± 0.22	200 ± 11	0.69 ± 0.017	0.78 ± 0.20
8	0.45 ± 0.039	1.6 ± 0.24	0.23 ± 0.036	15 ± 3.0	1.5 ± 0.27	7.8 ± 1.9	> 500	3.7 ± 1.0	4.2 ± 1.2
9	1.2 ± 0.19	1.4 ± 0.29	0.25 ± 0.043	7.9 ± 2.5	8.6 ± 1.5	9.1 ± 3.6	> 500	11 ± 0.64	1.8 ± 0.14
10	110 ± 17	> 500	770 ± 8.4	> 1000	650 ± 39	> 1000	> 1000	> 1000	> 1000
11	84[10]	32 ± 9.5	0.36[10]	> 500	> 500	> 500	440 ± 14	> 500	240 ± 11
12	< 0.010	> 5	0.065 ± 0.09	3.8 ± 0.57	0.19 ± 0.035	2.9 ± 0.49	120 ± 6.2	2.2 ± 0.20	0.46 ± 0.037
17	n.d.[a]	n.d.	0.98 ± 0.023	n.d.	n.d.	n.d.	120 ± 1.8	0.31 ± 0.006	n.d.
TDG[b]	24[8a]	340 ± 19	49[8a]	410 ± 21	980 ± 70	160[8a]	61[8a]	38[8a]	42 ± 1.1

[a] Not determined. [b] Thiodigalactoside.

basis of earlier analyses of **2** and **11**.[10] The substitution position preference of the fluorophenyl derivatives **3**–**5** ($m < p < o$) is reflected in the corresponding trifluoromethyl series **7**–**9**, albeit with somewhat higher K_d values.

Although the fluorophenyl-substituted **4** and **5** indeed reach low-nanomolar affinities for galectin-1, more noteworthy is the even higher affinity of the thiophen-3-yl compound **12**. This compound provided near quantitative inhibition at all concentrations tested, and no accurate dissociation constant could be reliably calculated. Hence, the dissociation constant could only be estimated as less than 10 nM, which is at least 2400 times better than the reference unsubstituted thiodigalactoside and natural disaccharide ligands.

In stark contrast, galectin-2 was inhibited with only micromolar K_d values by any of **2**–**12** and **17**. The best compound, the 2-fluorophenyl compound **3**, reached only a moderate affinity of about 1 μM, although this is nevertheless significantly better than that of the parent unsubstituted thiodigalactoside, reflecting the presence of positive interactions between **2**–**17** and this galectin.

Galectin-3 was strongly inhibited by several compounds and interestingly showed a selectivity profile similar to that of galectin-1; phenyl moieties carrying small substituents (**2**–**9**), as well as the thiophen-3-yl moiety (compound **12**), conferred high affinity, whereas phenyl groups bearing larger substituents (**10**, **11**), as well as the naphthyl group (compound **17**), were less efficiently bound by this galectin. A notable difference, however, is that whereas the biphenyl-substituted compound **10** is virtually detrimental to binding (as in the case of galectin-1), the 4-phenoxyphenyl-substituted compound **11** is reasonably well tolerated by galectin-3, with a sub-micromolar affinity, which is not the case for galectin-1. Hence, compound **11** displays, as reported earlier,[10] an important selectivity of more than 50-fold for galectin-3 over galectin-1. The reverse situation holds for thiophenyl **12**, which inhibits galectin-3, albeit with an affinity of 65 nM, but still less well than galectin-1. Hence, the thiophenyl derivative **12** has a clear selectivity for galectin-1 over galectin-3 and thus, through appropriate choice of aryl substituents on the triazole rings, selectivity for galectin-1 (by **12**) or galectin-3 (by **11**) is achieved.

Both CRDs of the tandem-repeat galectin-4 were evaluated. The N-terminal domain did recognize compounds **2**–**12** and **17** with moderate affinities in the low–medium micromolar range, which for all compounds is better than the parent thiodigalactoside. Reflecting the difference in fine specificity between the two galectin-4 domains, the C-terminal domain revealed mid-nanomolar affinities for several compounds. As observed for galectins-1 and -3, aryltriazoles carrying no or smaller substituents on the aryl moiety (**2**–**5** and **12**) were identified as the best inhibitors. Again, this suggests that one or both of the aryl-accommodating sites of galectin-4C can harbor only smaller structures. The 4-fluorophenyl derivative **5** stands out as a most potent inhibitor of galectin-4C with a K_d of 73 nM, which suggests a specific fluorine interaction and/or an ideal steric fit by the 4-fluoro substituent. Most likely, efficient inhibition of one domain[13] will be sufficient to block physiological/biological effects by galectin-4.

Galectin-7 binding is enhanced by the 4-aryltriazolyl groups of **2**–**9**, **12**, and **17**, whereas the sterically more demanding compounds **10**–**11** are virtually nonbinding. Similar observations were made for galectin-9N and -9C, which both bind several inhibitors with sub- to low-micromolar affinities. In contrast to galectin-4, no clear selectivity between the two domains of galectin-9 was observed.

Overall, the (4-aryltriazolyl)thiodigalactosides **2**–**12** and **17** delivered inhibitors significantly more potent than thiodigalactoside itself against galectins-1, -2, -3, -4N, -4C, -7, -9N, and -9C and more potent than the corresponding galactoside monosaccharide derivative against galectins-3, -7, and -9N (c.f., e.g., the monosaccharide corresponding to **2** shows K_d values of 150, 1700, and 1300 μM, respectively, against these three galectins[7a,8d]). In particular, galectins-1 and -3 were strongly inhibited, with several compounds showing low-nanomolar affinities. The inhibition potency against galectin-3 surpassed even that of our previously described corresponding 4-amidotriazolyl-[8d] and (4-aryltriazolyl)thiodigalactoside[10] derivatives. Several

compounds indeed possess a clear selectivity for these two galectins, whereas the selectivity between them is limited except in the cases of the thiophenyl derivative **12** and the phenoxy derivative **11** that displayed moderate selectivity for galectin-1 and galectin-3, respectively.

Structural studies

X-ray structures were conducted for three selected high-affinity compounds—the 3- and 4-fluorophenyl derivatives **4** and **5** and the thienyl derivative **12**—in complex with galectin-3. Initial refinements of X-ray diffraction data (1.5–1.6 Å resolution, Table S1 in the Supporting Information) produced clear differences in electron density within the galectin binding sites, revealing the bound ligands **4**, **5**, and **12** (Figure 1). In all cases, electron density is clearly evident for the thiodigalactoside cores of all three ligands **4**, **5**, and **12** (except for the solvent-orientated C6 hydroxy group), and for both triazole rings. The thiodigalactoside core of each of the ligands **4**, **5**, and **12** is in an identical binding mode to that observed in the previously reported galectin-3·thiodigalactoside complex[14] and forms identical protein–ligand interactions, thus confirming that they do not act as divalent ligands. Electron density is also defined

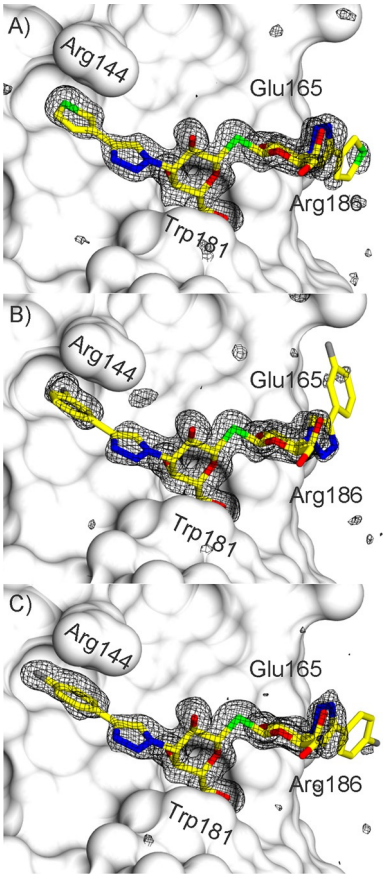

Figure 1. Difference electron density within the galectin-3 CRD binding sites showing bound A) **12**, B) **4**, and C) **5**. Difference electron density calculated from refinement with the ligand (stick representation) omitted from the model ($|F_o|-|F_c|\alpha_{calc}$; grey mesh, contoured at 3σ) and the protein represented by a gray solvent-accessible surface.

for the aromatic rings extending from one of the triazole C4 atoms of **4**, **5**, and **12** towards the Arg144 side chain. The second thiophene or fluorophenyl rings of the ligands **4**, **5**, and **12**, positioned above the salt bridge between Glu165 and Arg186, are less clearly defined on the initial difference electron density maps than the other parts of the ligands (upper region of the ligands in Figure 1 A–C). The positions of the thiophene ring of **12** and the 3-fluorophenyl ring of **4** are evident in the region near Glu165 and Arg186 in difference electron density maps when scaled to 2.5σ (calculated prior to addition of the ligand to the model), and refinements with the ligand included in the model show the thiophene and 3-fluorophenyl rings defined by $2mF_o-DF_c$ electron density when scaled at 0.7σ. Additional weak $2mF_o-DF_c$ electron density appears near Glu165 and Arg186 in the case of **4** after refinement, indicating a possible alternate conformation for the ring; however, the electron density is not clear enough to allow confident modeling of two alternate conformations for the ligand.

The 4-fluorophenyl ring of **5** near the Glu165–Arg186 salt bridge is poorly defined by the initial difference electron density. Refinement of the model with the ligand **5** in place, but excluding the 4-fluorophenyl ring near Glu165–Arg186, results in additional difference electron density that indicates the general location of the ring, and refinements with the ring included in the model resulted in weak $2mF_o-DF_c$ electron density (0.7σ) that supports the location of the ring. However, there is clearly a higher degree of disorder for this part of the ligand. This might initially appear counterintuitive because known ligands with aromatic groups near the Glu165–Arg186 salt bridge region of galectin-3 have shown enhanced affinities (e.g., the diamidothiodigalactosides[8a,b] and aromatic lactose 2-*O*-esters[15]). However, the interaction involves face-to-face stacking between the aryltriazole units and an extended surface of the π system of the Glu165–Arg186 ion pair, which could allow for the aryltriazole units to position themselves over different segments of the large π system with retained free energies of interaction.

The triazole rings of compounds **4**, **5**, and **12** located above His158 are each orientated with the nitrogen atoms positioned towards Trp181; this allows for the formation of a water-mediated hydrogen bond between N2 of the triazole and the nitrogen atom of Trp181 (Figure 2 A–C). The triazole rings of compounds **4**, **5**, and **12** located near the in-plane Glu165–Arg186 salt bridge show two alternate conformations that stack face-to-face to the salt bridge. In the complexes with **12** and **5**, the triazole nitrogen atoms are directed towards Glu165, whereas in the complex with **4** the ring is flipped, with the triazole nitrogen atoms close to Arg186. The orientation of one of the triazole rings in the cases both of **12** and of **5** results in contacts with both Glu184 and Arg186, whereas in the case of **4** the triazole is in contact with Arg186 only.

In all three galectin-3 complexes with **4**, **5**, and **12**, the ligand induces a conformational change in Arg144 (Figure 3) similar to that reported for the galectin-3 CRD structure in complex with a 3′-(2,3,5,6-tetrafluoro-4-methoxybenzamido)-LacNAc derivative (PDB ID: 1KJR).[7c] One of the terminal aro-

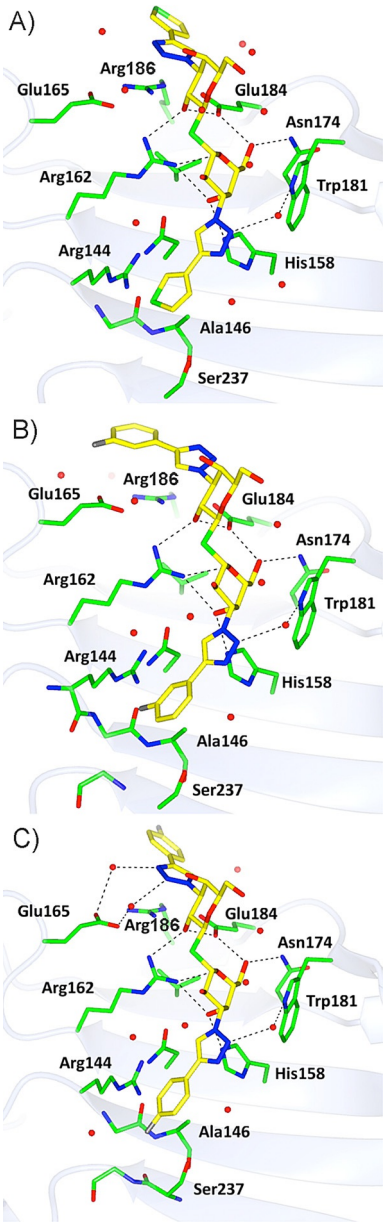

Figure 2. Galectin-3 CRD binding site interactions with A) **12**, B) **4**, and C) **5**. H-bond interactions between ligand (yellow bonds) and protein/water (green bonds) are shown as dashed lines.

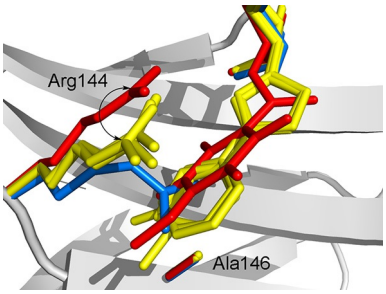

Figure 3. Superimposed view of the galectin-3 CRD binding site in the region of Arg144 for the complexes with **4**, **5**, and **12** (yellow), with the 3′-(2,3,5,6-tetrafluoro-4-methoxybenzamido) LacNAc derivative (red, PDB ID: 1KJR), and with lactose (blue, PDB ID: 3ZSJ).

matic rings of the ligands **4**, **5**, and **12** fits in each case into a pocket that is exposed by the Arg144 conformational change and moves away from the protein surface to form a face-to-face stacking interaction with Arg144 in a manner similar to that observed for the corresponding complex with the 3′-(2,3,5,6-tetrafluoro-4-methoxybenzamido)LacNAc derivative. However, in the structures of the complexes with **4**, **5**, and **12**, the additional length granted by the triazole linker allows the terminal aromatic rings to extend deeper into the pocket exposed by the movement of Arg144, which allows in each case for the formation of an additional contact with Ala146 that is not observed in the 3′-(2,3,5,6-tetrafluoro-4-methoxybenzamido)LacNAc complex. Additionally, although the conformational change of Arg144 in the complexes with **4**, **5**, and **12** is overall similar to that observed earlier for the 3′-(2,3,5,6-tetrafluoro-4-methoxybenzamido)LacNAc derivative,[7c] small differences are apparent. In the complexes with **4**, **5**, and **12** Arg144 has moved, relative to the complex with the 3′-(2,3,5,6-tetrafluoro-4-methoxybenzamido)LacNAc derivative (1.5–2.0 Å ζ-carbon to ζ-carbon distance), such that the guanidino group maintains its position directly above the aromatic ring of the ligand (Figure 3). One thiophene ring of **12** is orientated to bury the sulfur atom deeply in the pocket exposed by the movement of Arg144, as is the fluorine atom in the 3-fluorophenyl ring of **4**. The single-wavelength anomalous dispersion log-likelihood gradient (SAD LLG) map calculated for the complex with **12** confirms the orientation of the thiophene ring, showing a clear peak positioned at the location of the sulfur atom within the pocket near Arg144. The fluorine atom of **4** below Arg144 is situated at distances of 3.9 and 3.4 Å, and at angles of 155 and 147°, from the backbone carbonyl groups of Arg144 and Ile145, respectively; this suggests the formation of two orthogonal multipolar interactions.[16] The fluorine atom of the 4-fluorophenyl ring in the complex with **5** is directed towards Gly238 and Ser237 and makes contact with the α-carbon of Gly238 and is also positioned well for forming an orthogonal dipolar interaction with the Ser237 carbonyl group (distance 3.6 Å and angle 140°). Furthermore, the guanidinium ion of the arginine side chain has been proposed to be highly fluorophilic, because fluorine atoms in fluorinated pharmaceuticals have been observed to reside close to guanidinium moieties in proteins.[16a,17] Finally, fluorination typically results in increased lipophilicity,[16a,17] and fluorinated hydrocarbons are in general poorly solvated in water;[18] this would support a conclusion that burying fluorinated lipophilic ligand parts is important for achieving high affinity of **4** and **5** for galectin-3. The equivalent of Arg144 is absent in some galectins;[19] consequently, targeting ligand interactions to this region and engaging Arg144 through cation–π interactions is proposed as a means of enhancing galectin binding selectivity.

Galectin-3 mutant studies

The X-ray structures of the galectin-3 complexes revealed that the aryltriazole units of **4**, **5**, and **12** stacked face-to-face onto two (Arg144 and Arg186) arginine guanidinium groups. In the case of galectin-3, the two 3-fluorophenyl moieties of **4** have

different stacking modes with Arg144 and Arg186: one 3-fluorophenyl moiety is stacked on top of the Arg186 guanidinium group, whereas the other 3-fluorophenyl moiety is inserted between the protein surface (backbone) and the Arg144 guanidinium group (Figures 1B, 2B, and 3). In order to achieve further understanding about the nature of the aryltriazole–arginine stacking interactions, we determined the affinity of **4** towards four galectin-3 mutants: R144K, R144S, R186K, and R186S (Table 2). The R144S and R186S mutants were chosen because the side chain is removed without introduction of a very nonpolar surface whereas the R144K and R186K mutants were chosen because the cationic nature of the side chain is retained while the planar π system of the guanidino group is removed.

Table 2. Dissociation constants for **4** from galectin-3 variants as determined by a competitive fluorescence anisotropy assay.[12]

Dissociation constant [μM]				
wt	R144K	R144S	R186K	R186S
0.014 ± 0.003	0.041 ± 0.0045	0.017 ± 0.0032	0.54 ± 0.039	1.0 ± 0.12

The effect of the R144S mutant is minimal, which suggests that the stacking of Arg144 onto the 3-fluorophenyl group of **4** does not contribute significantly to the free energy of binding, whereas the surface complementarity and the interactions between the 3-fluorophenyl group and the rest of the protein surface remain essentially unchanged.

The R144K mutant binds **4** only about three times less well than the wild type; this suggests that the lysine side chain, like an arginine side chain, can form cation–π interactions. However, unlike the arginine guanidine group, the lysine amino group obviously lacks a π system, and π-stacking capability might be the reason why the interaction with the 3-fluorophenyl group of **4** is possibly slightly less productive.

The R186S mutant shows a large drop in affinity for **4**, clearly revealing that a 3-fluorophenyl stacking interaction onto Arg186 is an important contributor to the high affinity of **4** for galectin-3. The Arg186 side-chain guanidinium ion, in contrast to the Arg144 side chain, is involved in an extensive network of in-plane bifurcated ion-pairs (Figure 2), which form an extended π system surface onto which a 3-fluorophenyl group stacks, in analogy with, for example, the acetamido group of *N*-acetyllactosamine[7c] and the aromatic rings of 2-*O*-benzoyllactose derivatives.[15] In the mutant R186S this extended π system of bifurcated ion-pairs is interrupted, and the 3-fluorophenyl unit cannot form a beneficial stacking interaction. Instead, a poorly solvated cavity with poor complementarity to the 3-fluorophenyl group of **4** is present.

Some binding affinity is regained in the R186K mutant, relative to the R186S mutant. This is presumably due to the capability of the lysine side chain at least partially to substitute and stabilize the Arg186 side chain's key π-system-forming ion pairing with the two surrounding Glu165 and Glu184 residues, as well as providing similar surface complementarity to the 3-fluorophenyl group of **4**.

In short, it can be hypothesized that the high affinities of (4-aryltriazolyl)thiodigalactosides such as **4**, **5**, and **12** towards galectin-3, according to X-ray structural analysis of galectin-3 complexes and galectin-3 mutant studies, arise as a result of several factors. Firstly, ideal surface complementarity between the proteins and ligands (Figure 1) are, not unexpectedly, critical because this maximizes dispersion forces and presumably also beneficial desolvation effects. Stacking interactions between the galectin's arginine side chain guanidinium functionalities and the ligands' phenyltriazole moieties are probably important, as are fluorine orthogonal dipolar interactions[16c] with backbone carbonyl groups. Hence, whereas the core thiodigalactoside disaccharide mimics natural disaccharide ligand fragments (e.g., lactose and LacNAc) in terms of affinity contributions and structure, the appended noncarbohydrate aryltriazole moieties engage in galectin–ligand interactions not seen in natural lectin·ligand complexes (i.e., predominantly hydrogen bonding and CH–π interactions), resulting in drastic affinity enhancements and enhanced selectivities.

Low-nanomolar galectin antagonists having been discovered, an important question of their efficiency for antagonizing galectin–glycoprotein interactions in biological systems was addressed with compound **4** in two models. Firstly, an in vitro cell assay was developed with the goal of gaining new knowledge about the putative intracellular glycan-binding activities of galectin-3 and possible effects in cells challenged with vesicle-damaging agents. The second model was intended to achieve further understanding of, as well as to quantify, the effects of antagonizing galectin-3 in an in vivo mouse model of bleomycin-induced idiopathic pulmonary fibrosis.[6b]

Intracellular inhibition by galectin-3 antagonist 4 in an amitriptyline-induced vesicle damage assay

Galectin accumulation around damaged vesicles in response to challenge by bacteria or chemical agents has been demonstrated in several studies, and the formation of galectin-3[20] or galectin-8[21] puncta has been proposed as a new marker for vesicular insult, regardless of the insult being of bacterial[20b,21] or chemical origin.[20a] Galectin-3 accumulation around damaged vesicles has, in addition, been shown to depend on glycan-binding, either by knock-down of certain glycosyltransferases[20b] or through knock-in of a galectin-3 mutant (R186S) with severely reduced affinity for endogenous glycans.[20a] Antagonizing effects on such glycan-binding-dependent galectin-3 events on damaged vesicles[20b] could provide qualitative information on intracellular availability and activity of antagonists, such as compound **4**. Cationic amphiphilic drugs, including the tricyclic antidepressant amitriptyline, induce phospholipidosis, and it is speculated that they accumulate in acidic lysosomes and induce vesicle damage in tumor cell lines.[20a,22] We postulated that treatment of cells with amitriptyline would induce formation of galectin-3 puncta in a fashion similar to that shown by other vesicular damaging agents, such as glycyl-L-phenylalanine 2-naphthylamide[21] and L-leucyl-L-leucine methyl ester.[20a] Amitriptyline has the advantage of being more stable under the experimental conditions used and does

not degrade in solution like, for example, glycyl-L-phenylalanine 2-naphthylamide. Furthermore, amitriptyline does not require the use of DMSO as co-solvent for solubilization, which is needed for the more commonly used peptidic vesicular damaging agents.

Indeed, treatment of breast carcinoma MCF-7 cells with amitriptyline resulted in distinct accumulation of galectin-3 into vesicle-associated puncta, hypothetically within galectin-3:glycoprotein lattices, in a dose-dependent manner (Figure 4A and B). Co-treatment with 10 μM compound **4** and 10 or 50 μM amitriptyline resulted in a significant reduction in the number of galectin-3 dots relative to amitriptyline treatment alone (Figure 4A and B), and this strongly supports the conjecture that compound **4** can act as an intracellular antagonist for galectin-3 in cell culture systems. The experimental concentration of **4** was selected to achieve a significant effect and possibly reflects a relatively slow cellular uptake and intracellular concentration increase of **4** sufficient to block intracellular galectin-3.

Pharmacological intervention in a bleomycin-induced lung fibrosis mouse model

Galectin-3 has been shown to promote both macrophage M2 polarization[5b] and myofibroblast activation:[6b] that is, in two key profibrotic cell types. In the case of macrophage M2 polarization, galectin-3 association with CD98 on the macrophage cell surface, presumably within lattices, was shown to be a plausible molecular mechanism for regulating M2 activation through phosphatidylinositol 3-kinase (PI3K) activation.[5b] Analogously, transforming growth factor-β (TGF-β) receptor II has been shown to bind galectin-3 on cell surfaces; this was suggested to be a critical molecular mechanism for inducing myofibroblast activation.[6b] Furthermore, in vivo an intratracheal single dose of the galectin-3 antagonist **4** (10 μg per mouse, 500 μg kg^{-1}) was demonstrated to display an antifibrotic effect in a bleomycin-induced lung fibrosis mouse model.[6b] Hence, it can be hypothesized that compound **4** exerts dual antifibrotic effects by disrupting lattices with CD98 on M2 macrophages and with TGF-β-RII on myofibroblasts and associated profibrotic signaling. However, the single-dose experiment left unanswered questions concerning the in vivo dose/response efficacy of compound **4** and how this compared to those of alternative antifibrotic agents. Hence, we conducted a dose/response study of therapeutic administration of compound **4** in this model, in comparison with pirfenidone, one of only two recently approved drugs for treating idiopathic pulmonary fibrosis (IPF). Mice ($n=8$) received bleomycin sulfate (1.65 mg kg^{-1} intratracheally), resulting in inflammation and subsequent fibrosis development, followed either by 200 mg kg^{-1} pirfenidone twice daily orally from days 18–24 or by compound **4** at 500, 150, 50, or 5 μg kg^{-1} intratracheally as a single administration every second day (days 18, 20, 22, and 24). Lung collagen content and histopathology was determined on day 26. Pirfenidone (200 mg kg^{-1}) significantly reduced bleomycin-induced collagen accumulation from (670 ± 77) to (375 ± 53) μg collagen per lobe ($p<0.01$), as did 500 and 150 μg kg^{-1} of compound **4** [(355 ± 46) and (546 ± 22) μg collagen per lobe $p<$

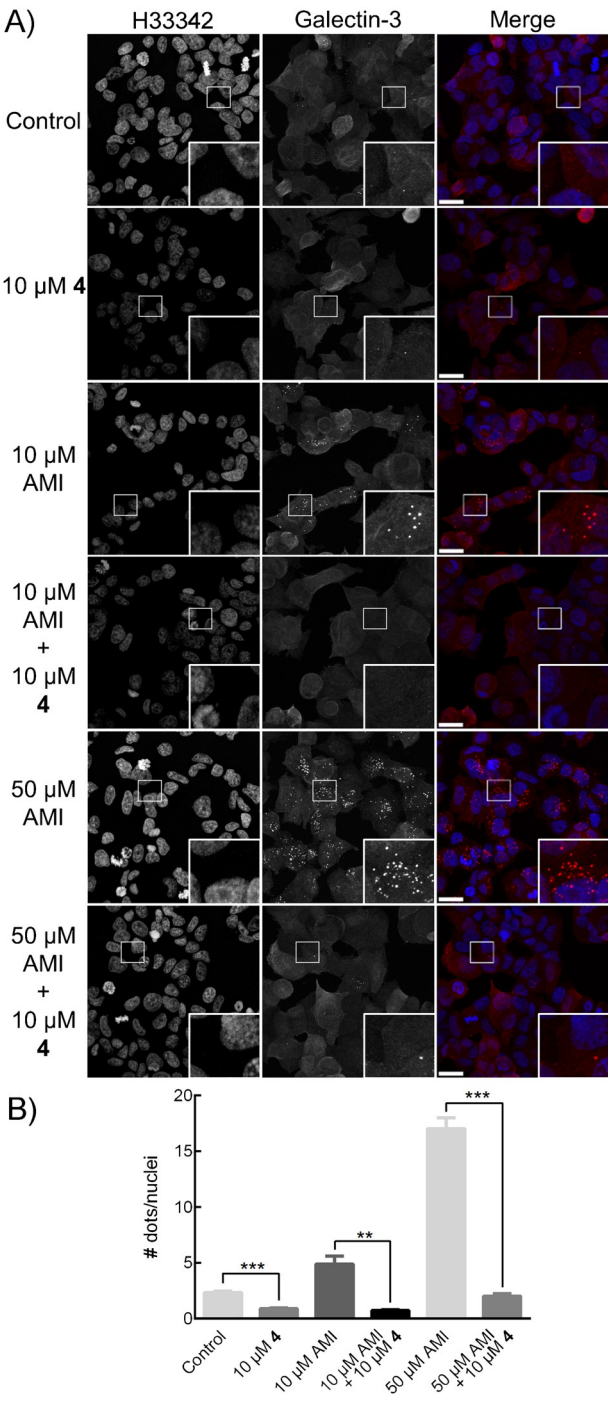

Figure 4. Inhibition of galectin-3 accumulation around amitriptyline-damaged (AMI-damaged) vesicles in MCF-7 cells. Cells were treated with combinations of 10 μM compound **4** and 10 or 50 μM amitriptyline for 24 h; control cells were treated with 0.1% (*v*/*v*) DMSO. A) Galectin-3 staining was visualized with anti-rat Alexa Fluor 594 (red), whereas Hoechst 33342 (blue) was used to stain the nuclei. The immunofluorescence pictures displayed are representative for each treatment. Scale bars: 20 μm. Small square inserts show areas magnified in each large square insert. B) The numbers of galectin-3 dots were counted manually with use of ImageJ in four different images for each set of experimental conditions, and are given as mean ± SEM. Each data set represents ≈250 cells. $^{**}p<0.01$, $^{***}p<0.001$, Student's t-test.

0.01, $p < 0.03$, respectively, Figure 5]. In addition, compound **4** at 500 and 150 μg kg^{-1} doses and pirfenidone significantly decreased the fibrosis score. Hence, when delivered directly into the lung, compound **4** achieves efficacy at much lower concentrations than orally delivered pirfenidone. The lower dose needed with administration of **4** could be due to the, not unexpectedly, improved lung targeting by intratracheal administration in combination with the high affinity of **4** for the target galectin-3 protein, shown to be a key regulator of fibrosis biochemistry. Lung availability of an orally administered compound is likely to be lower than that of an intratracheally administered compound, which might at least partly explain the need for a higher dose of oral pirfenidone to achieve the same efficacy as intratracheal **4**. In addition, compound **4** did not reduce protein in the BAL (bronchoalveolar lavage) fluid—an indication of vascular leakage—but both pirfenidone and compound **4** reduced MCP-1 (monocyte chemoattractant protein-1) levels (Figure 6). Compound **4** did not produce any clear significant decrease in galectin-3 levels in BAL fluid or serum. The absence of a significant decrease in galectin-3 levels in BAL fluid is likely due to the fact that BAL fluid samples are from whole lung and not only the fibrotic area. Because non-fibrotic tissue has a background expression of galectin-3 this will influence the total galectin-3 levels in BAL fluid samples, so BAL fluid galectin-3 analysis might be underestimating the actual concentration of galectin-3 in the diseased areas of the lung.

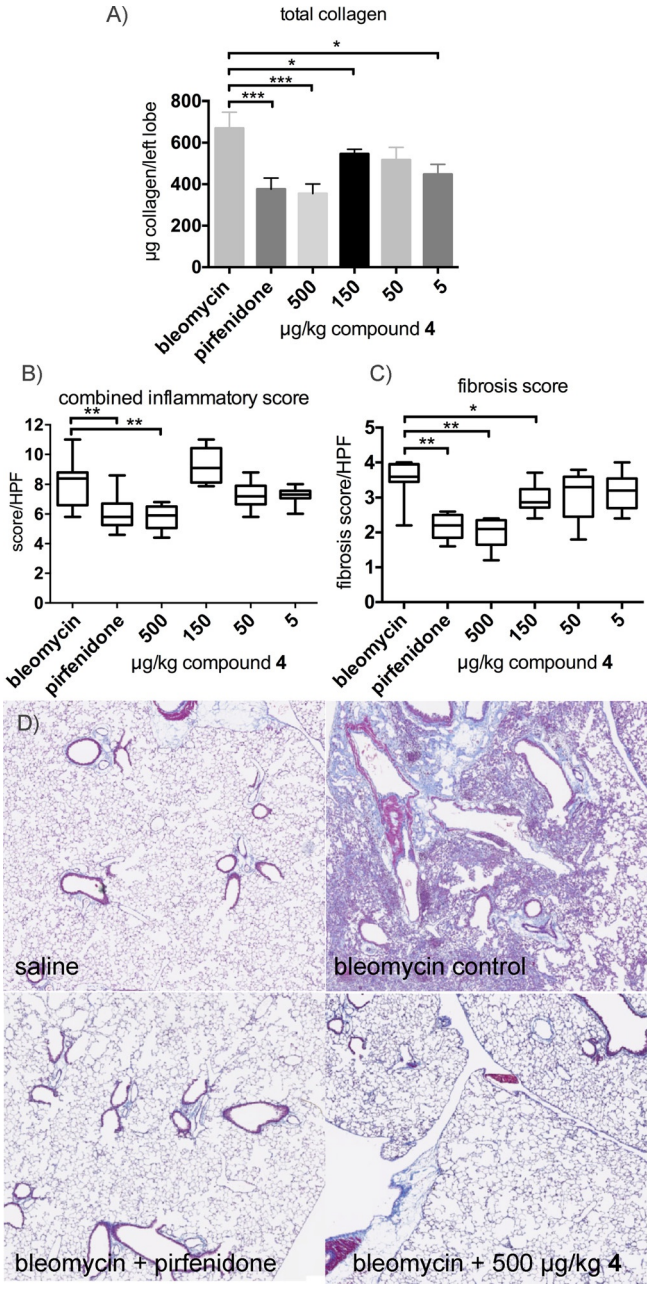

Figure 5. Effects of pirfenidone and **4** on bleomycin-induced lung fibrosis in mice. A) Total lung collagen, B) histological inflammatory score, and C) histological fibrosis score. Results represent the means ± SEMs of $n = 8$ mice per group. (* $p < 0.03$, ** $p < 0.05$, *** $p < 0.01$ statistically different from bleomycin control). D) Representative stained (Masson's trichrome) sections of mouse lung from uninjured saline control, bleomycin control, and bleomycin treated with oral pirfenidone (200 mg kg^{-1}) or intratracheal **4** (500 μg kg^{-1}).

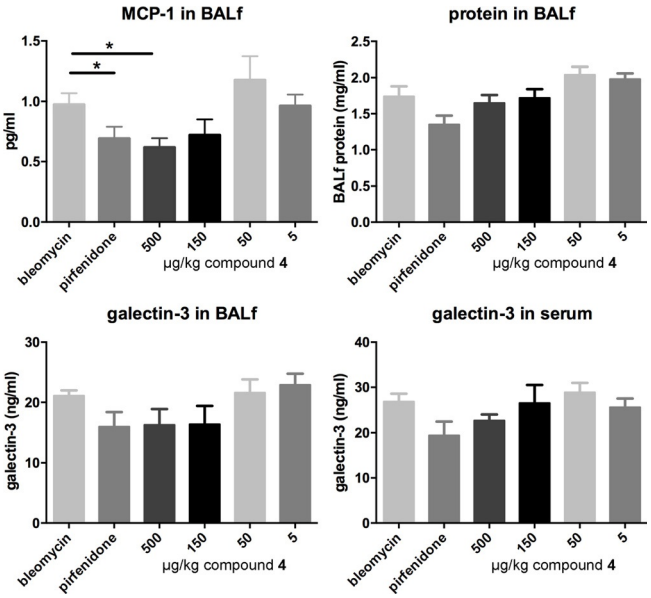

Figure 6. Effects of pirfenidone and compound **4** on BAL fluid parameters in bleomycin-induced lung fibrosis in mice. Total protein measured by BCA reagent, MCP-1, and galectin-3 in BAL fluid and serum were measured by ELISA. Results represent the means ± SEMs of $n = 8$ mice per group. (* $p < 0.05$, statistically different from bleomycin control).

Conclusion

Highly potent galectin-1 and -3 antagonists were discovered through synthesis, optimization, and structural analysis of doubly C3-aryltriazolyl-substituted thiodigalactosides. Low-nanomolar affinities towards galectins-1 and -3 were achieved, and some compounds displayed selectivity for individual galectins. Structural and mutational studies showed evidence that the exceptional affinity enhancement originated largely from the aryltriazole moieties forming stacking interactions with protein π systems (arginine side chains unpaired or ion-paired

with glutamate or aspartate carboxylates) and in some cases fluorine-derived orthogonal multipolar interactions that endogenous glycoconjugate glycans do not form. The nature of the aryltriazole moieties has a significant influence over galectin subtype selectivities, which could also be explained in terms of small, but significant, differences revealed in the structural studies. Overall, the results corroborate the promising strategy for discovery of high-affinity and selective lectin antagonists by exploring non-carbohydrate structural elements that form interactions with lectins that glycoside fragments of endogenous glycoconjugate ligands do not. Hence, drug development targeting lectins need not necessarily involve a strategy of multimerizing ligands and antagonists to achieve sufficient affinities, and the major challenges relating to pharmacokinetics, bioavailability, and toxicity/immunogenicity associated with multivalent antagonists might be avoidable.

One antagonist—compound **4**—was observed to have intracellular availability and activity as it blocked amitriptyline-induced vesicle damage in breast carcinoma MCF-7 cells. Although the question of which glycoprotein binding partner is involved in the galectin-3 accumulation on damaged vesicles still remains to be answered, the lysosome-associated membrane proteins LAMP-1 and LAMP-2 might be candidates for this role because they have been shown to be galectin-3 ligands on the surfaces of tumor cells[23] and are thus possible candidate glycoprotein ligands in our model. Importantly, these observations suggest that intracellular galectin-3–glycoprotein-binding events occur and might be biologically relevant. Targeting such interactions with synthetic antagonists might be a viable strategy, although PK-ADMET properties obviously have to be improved for intracellular/systemic availability and therapeutic applications.

Furthermore, intratracheally delivered compound **4** attenuated bleomycin-induced lung fibrosis in a mouse model in a dose-dependent manner and possessed efficacy at significantly lower doses than the approved oral antifibrotic pirfenidone and thus compared favorably with pirfenidone. This might further support a dual molecular mechanistic hypothesis in which galectin-3-promoted macrophage and myofibroblast activation results in sustained profibrotic cell signaling and scar formation.

Finally, five-membered aromatic heterocycles are common structural elements in many drugs, and 1,2,3-triazoles in particular are readily synthesized. This makes the compounds reported here promising leads for the development of new galectin-targeting therapeutics that disrupt cellular signal-sustaining galectin-3 lattices, as well as highly valuable tools for studying galectin biology and molecular mechanisms.

Experimental Section

Expression constructs, expression, and purification of recombinant galectins: Human galectin-1,[24] galectin-2,[25] galectin-3,[26] galectin-4N,[12a] galectin-4C,[12a] galectin-8N,[13b] and mouse galectin-7[27] were expressed and purified as described earlier. Human galectin-9N and galectin-9C were produced in *E. coli* BL21Star (DE3) cells (Invitrogen) and purified by affinity chromatography on lactosyl-Sepharose essentially as described for galectin-8.[13b] DNAs encoding the genes of human galectin-9N and galectin-9C were cloned into the pET-32 Ek/LIC vector (Novagen, Madison, WI) according to the manufacturer's instructions. Briefly, I.M.A.G.E. clone 2208156 (American Type Culture Collection) was used as template together with the following polymerase chain reaction (PCR) primers. The vector used for galectin-9N encoded the N-terminal 170 amino acids of galectin-9 and thioredoxin with the primers forward: 5′-GACGAC GACAAG ATGATG GGTTCA GCGGTT CCCAGG-3′, forward 2: 5′-GAGGAG AAGCCC GGTTCA GGAAAC AGACAG GCTGGG AGAACG GC-3′, and reverse: 5′-GAGGAG AAGCCC GGTGCC GCCTAT GTCTGC ACATGG G-3′. The vector used for galectin-9C encoded the *C*-terminal amino acids 205–355 of galectin-9 and thioredoxin with the primers forward: 5′-GACGAC GACAAG ATGGGA CAGATG TTCTCT ACTCCC-3′ and reverse: 5′-GAGGAG AAGCCC GGTGCG GCCTAT GTCTGC ACATGG G-3′. The bacteria were grown (37 °C, 200 rpm) in lysogeny broth (LB) with ampicillin (1 mg L^{-1}) overnight, followed by induction with isopropyl thio-β-D-galactoside (IPTG, 1 mM) for 4 h (29 °C, 200 rpm). The culture was centrifuged (4000 *g*, 15 min, 4 °C), and the pellet was dissolved in MEPBS [phosphate-buffered saline with EDTA (2 mM) and β-mercaptoethanol (4 mM), 50 mL] and sonicated for 10–20×30 s on ice. The sonicated bacteria were centrifuged (17000 *g*, 30 min, 4 °C), and the supernatant was subjected to affinity chromatography with a lactosyl-Sepharose column washed with MEPBS and a pre-elution of lactose (7.5 mM). The bound proteins were eluted with Lac-MEPBS [MEPBS with lactose (150 mM)] as elution buffer. Lactose was removed by chromatography on a PD-10 column (Amersham Biosciences) with repeated ultrafiltration with Centriprep (Amicon).

Competitive fluorescence polarization experiments to determine galectin affinities: Fluorescence polarization experiments were performed either with a POLARStar plate reader and FLUOstar Galaxy software or with a PheraStarFS plate reader and PHERAstar Mars version 2.10 R3 software (BMG, Offenburg, Germany) and fluorescence anisotropy of fluorescein-tagged probes measured with excitation at 485 nm and emission at 520 nm. K_d values were determined in PBS as previously described[12,28] with specific conditions for each galectin as described below. Compounds **3**–**10** were dissolved in neat DMSO at 100 mM and diluted in PBS to three to six different concentrations to be tested in duplicate. Average K_d values and SEMs were calculated from 4 to 25 single-point measurements showing between 30–70% inhibition.

Galectin-1 affinities: Experiments were performed at 20 °C with galectin-1 at 0.50 μM and the fluorescent probe 3,3′-dideoxy-3-[4-(fluorescein-5-yl-carbonylaminomethyl)-1*H*-1,2,3-triazol-1-yl]-3′-(3,5-dimethoxybenzamido)-1,1′-sulfanediyl-di-β-D-galactopyranoside[24] at 0.10 μM.

Galectin-2 affinities: Experiments were performed at 20 °C with galectin-2 at 10 μM and the fluorescent probe 3,3′-dideoxy-3-[4-(fluorescein-5-yl-carbonylaminomethyl)-1*H*-1,2,3-triazol-1-yl]-3′-(3,5-dimethoxybenzamido)-1,1′-sulfanediyl-di-β-D-galactopyranoside at 0.10 μM.

Galectin-3 affinities: Experiments were performed at 20 °C with galectin-3 at 0.20 μM and the fluorescent probe 3,3′-dideoxy-3-[4-(fluorescein-5-yl-carbonylaminomethyl)-1*H*-1,2,3-triazol-1-yl]-3′-(3,5-dimethoxybenzamido)-1,1′-sulfanediyl-di-β-D-galactopyranoside at 0.02 μM or with galectin-3 at 1.0 μM and 2-(fluorescein-5/6-yl-carbonyl)aminoethyl 2-acetamido-2-deoxy-α-D-galactopyranosyl-(1–3)-[α-L-fucopyranosyl-(1–2)]-β-D-galactopyranosyl-(1–4)-β-D-glucopyranoside[12] at 0.10 μM.

Galectin-4N affinities: Experiments were performed at 20 °C with galectin-4N at 3.0 μM and the fluorescent probe 3,3′-dideoxy-3-[4-(fluorescein-5-yl-carbonylaminomethyl)-1*H*-1,2,3-triazol-1-yl]-3′-(3,5-dimethoxybenzamido)-1,1′-sulfanediyl-di-β-D-galactopyranoside at 0.10 μM.

Galectin-4C affinities: Experiments were performed at 20 °C with galectin-4C at 0.50 μM and the fluorescent probe 2-(fluorescein-5/6-yl-carbonyl)aminoethyl 2-acetamido-2-deoxy-α-D-galactopyranosyl-(1–3)-[α-L-fucopyranosyl-(1–2)]-β-D-galactopyranosyl-(1–4)-β-D-glucopyranoside at 0.1 μM.

Galectin-7 affinities: Experiments were performed at 4 °C with galectin-7 at 2.00 μM and the fluorescent probe β-D-galactopyranosyl(1–4)-2-acetamido-2-deoxy-β-D-glucopyranosyl(1–3)-β-D-galactopyranosyl(1–4)-(*N*1-fluorescein-5-yl-carbonylaminomethylcarbonyl)-β-D-glucopyranosylamine[29] at 0.1 μM.

Galectin-8N affinities: Experiments were performed at 20 °C with galectin-8N at 0.40 μM and the fluorescent probe 2-(fluorescein-5-yl-carbonylamino)ethyl β-D-galactopyranosyl(1-4)-2-acetamido-2-deoxy-β-D-glucopyranosyl(1–3)-β-D-galactopyranosyl(1–4)-β-D-glucopyranoside[13b] at 0.1 μM.

Galectin-9N affinities: Experiments were performed at 20 °C with galectin-9N at 1.0 μM and the fluorescent probe 2-(fluorescein-5-yl-carbonylamino)ethyl β-D-galactopyranosyl(1–4)-2-acetamido-2-deoxy-β-D-glucopyranosyl(1–3)-β-D-galactopyranosyl(1–4)-β-D-glucopyranoside at 0.1 μM.

Galectin-9C affinities: Experiments were performed at 20 °C with galectin-9C at 2.0 μM and the fluorescent probe 3,3′-dideoxy-3-[4-(fluorescein-5-yl-carbonylaminomethyl)-1*H*-1,2,3-triazol-1-yl]-3′-(3,5-dimethoxy-benzamido)-1,1′-sulfanediyl-di-β-D-galactopyranoside at 0.10 μM.

Galectin-3 R144S affinities: Experiments were performed at 20 °C with galectin-3 R144S at 0.30 μM and the fluorescent probe 2-(fluorescein-5/6-yl-carbonyl)aminoethyl 2-acetamido-2-deoxy-α-D-galactopyranosyl-(1–3)-[α-L-fucopyranosyl-(1–2)]-β-D-galactopyranosyl-(1–4)-β-D-glucopyranoside at 0.02 μM.

Galectin-3 R144K affinities: Experiments were performed at 20 °C with galectin-3 R144K at 0.40 μM and the fluorescent probe 2-(fluorescein-5/6-yl-carbonyl)aminoethyl 2-acetamido-2-deoxy-α-D-galactopyranosyl-(1–3)-[α-L-fucopyranosyl-(1–2)]-β-D-galactopyranosyl-(1–4)-β-D-glucopyranoside at 0.02 μM.

Galectin-3 R186S affinities: Experiments were performed at 20 °C with galectin-3 R186S at 3.50 μM and the fluorescent probe 2-(fluorescein-5/6-yl-carbonyl)aminoethyl 2-acetamido-2-deoxy-α-D-galactopyranosyl-(1–3)-[α-L-fucopyranosyl-(1–2)]-β-D-galactopyranosyl-(1–4)-β-D-glucopyranoside at 0.1 μM.

Galectin-3 R186K affinities: Experiments were performed at 20 °C with galectin-3 R186K at 0.90 μM and the fluorescent probe β-D-galactopyranosyl(1–4)-2-acetamido-2-deoxy-β-D-glucopyranosyl-(1–3)-β-D-galactopyranosyl(1–4)-(*N*1-fluorescein-5-yl-carbonylaminomethylcarbonyl)-β-D-glucopyranosylamine at 0.1 μM.

Crystallization: Compounds **4**, **5**, and **12** were prepared under the galectin-3 crystallization conditions by initial solubilization in poly(ethylene glycol) (PEG 6000, 55%, *w/v*), before addition of other crystallization reagents to give a final concentration of 20 mM of **4**, **5**, or **12** under the galectin-3 crystallization condition [PEG 6000 (31%, *w/v*), Tris·HCl (pH 7.5, 100 mM), $MgCl_2$ (100 mM) for galectin-3]. Galectin-3-CRD lactose or galactose co-crystals (prepared as previously described[30]) were soaked for 2–8 days in drops containing a 1:1 ratio of the ligand-containing crystallization solution and human galectin-3-CRD (20 mg mL^{-1}) in Tris·HCl [pH 7.5, 10 mM (pre-equilibrated co-crystallization drops that had not produced crystals)].

X-ray diffraction analysis and structure determination: X-ray diffraction data sets were collected at room temperature from human galectin-3-CRD crystals mounted in 0.7 mm quartz capillaries with a ProteumR (Bruker AXS) diffractometer and MacScience M06X^{CE} rotating-anode generator (wavelength 1.5418 Å) equipped with a SMART6000 CCD detector. X-ray diffraction data were integrated by using SAINT (Bruker AXS) and scaled and merged by using SCALA[31] in the CCP4 suite of crystallographic software.[32] Structures were solved by initial rigid body refinement with use of a previously published galectin-3-CRD structure (PDB ID: 1A3K),[33] with ligand and waters removed, as the initial model. Translation/libration/screw (TLS) and restrained refinement were performed with REFMAC5.[34] Anomalously scattering elements were identified with the aid of single-wavelength anomalous dispersion log-likelihood gradient maps (SAD LLG maps); calculated by use of Phaser[35] (in experimental phasing mode in CCP4) in the "SAD with molecular replacement partial structure" mode with purely anomalous scatterers and zero LLG-map completion cycles and the current model and F+ and F− structure factor amplitudes as input. Visualization of electron density and model building was performed with Coot.[36] Ligand geometry topologies for refinement were initially created by REFMAC5 within CCP4 (LIBCHECK) or by using the Dundee PRODRG2 Server.[37] In most cases minor to moderate manual editing of the automatically generated topologies was performed to ensure correct atom and bond types. Model validation and analysis was performed with MolProbity.[38] Figures were created with the aid of the CCP4 molecular-graphics project (CCP4MG).[39]

Accession codes: The atomic coordinates and structure factors of galectin-3 in complex with **4**, **5**, and **12** have been deposited with the Protein Data Bank under accession codes 5E89, 5E8A, and 5E88, respectively.

Site-directed mutagenesis: Mutants of human galectin-3 were made by using the QuickChange II site-directed mutagenesis kit (Stratagene), produced in *E. coli* BL21Star(DE3) cells (Invitrogen) and purified by affinity chromatography on lactosyl-Sepharose as previously described.[40] Mutagenic primers for PCR were as follows: Gal-3R186K (AGA→AAA) sense (5′-CTGGGG AAGGGA AGAAAA ACAGTC GGTTTT CCC-3′) and antisense (5′-GGGAAA ACCGAC TGTTTT TCTTCC CTTCCC CAG-3′) and Gal-3R144K (AGA→AAA) sense (5′-GAAGCC CAATGC AAACAA AATTGC TTTAGA TTTCCA AAGAG-3′) and antisense (5′-CTCTTT GGAAAT CTAAAG CAATTT TGTTTG CATTGG GCTTC-3′). Successful mutagenesis was confirmed by sequencing by GATC Biotech (Konstanz, Germany) in the forward direction from the T7 promotor primer and in the reverse direction from the pET-RP primer. Galectin-3 R144S and R186S were prepared as reported earlier.[40]

Cell culture and immunocytochemistry: MCF-7 cells were maintained in RPMI-1640 (Biochrom, Berlin, Germany) supplemented with fetal bovine serum (Biochrom, Berlin, Germany, 10%), insulin (Sigma–Aldrich, 10 μg mL^{-1}), streptomycin (100 μg mL^{-1}), and penicillin (Hyclone, 100 U mL^{-1}). The cells were kept in a 37 °C humidified incubator supplied with CO_2 (5%) in air. For the experiments, stock solutions of compound **4** (4 mM) in DMSO (40%) were used, whereas for amitriptyline (Sigma–Aldrich) stock solutions (20 mM) were made in sterile water. Both compound **4** and amitriptyline were serially diluted in RPMI-1640 before treatment of cells, such

that the DMSO concentration did not exceed 0.1% (*v/v*). MCF-7 (10^5 cells) were seeded onto sterile coverslips (placed in multiwell plates) and cultured for 24 h. Cells were then treated with amitriptyline (either 10 or 50 μM) either alone or in combination with compound **4** (10 μM) for 24 h. After fixation with paraformaldehyde (2%) in phosphate-buffered saline (PBS) for 10 min, cells were permeabilized with Triton X-100 (0.4%, *v/v*) in PBS for 5 min. Nonspecific binding was inhibited by blocking the cells with blocking buffer [BSA (1%, *w/v*), Tween 20 (0.1%, *v/v*) in PBS] for 10 min. Cells were then incubated with rat anti-mouse galectin-3 antibody (anti-Mac-2[41]) in a humidified chamber for 1 hour at room temperature. After three washes with PBS, goat anti-rat Alexa Fluor 594 (Invitrogen) was added. Hoechst 33342 (10 ng mL^{-1}) was used to stain the nuclei. Cells were visualized by obtaining z-stacks of high-magnification single optical planes with a LSM510 confocal laser scanning microscope (Carl Zeiss), conjugated with a Hamamatsu R6357 (Hamamatsu Photonics K. K., Hamamatsu, Japan) photomultiplier. Galectin-3 dots were counted manually by using ImageJ 1.47v and the plug-in Cell Counter (Wayne Rasband, National Institutes of Health, USA). Bar graphs representing galectin-3 dots/nuclei are expressed as mean values of different image areas ± SEMs. For measuring statistical significance between a pair of data sets, Student's t-test (two tailed, unpaired) was employed. $p < 0.05$ was considered to be significant.

Bleomycin-induced fibrosis: Bleomycin was purchased from Apollo Scientific and reconstituted in sterile saline at a concentration of 0.66 mg mL^{-1}. Aliquots were stored at −20 °C. Pirfenidone was purchased from Tocris Biochemicals and was dissolved in carboxymethyl cellulose (Sigma–Aldrich, 0.5%) to a concentration of 20 mg mL^{-1}. Compound **4** was dissolved in DMSO (100%) at a concentration of 10 mg mL^{-1}, and aliquots were stored at −20 °C. For each day, compound **4** for instillation was diluted in sterile saline to give a final concentration of DMSO in the instillate of 2%. Female C57/Bl6 mice of ten weeks of age were purchased from Charles River and were maintained in 12 h light/12 h dark cycles with free access to food and water. All procedures were performed in accordance with Home Office guidelines [Animals (Scientific Procedures) Act 1986].

Mice were randomized into eight treatment groups ($n = 8$) and were anesthetized with isofluorane. Bleomycin (33 μg) in sterile saline (50 μL) was instilled into the lungs. A control group received sterile saline (50 μL). Mice were monitored closely over the next 26 days. Pirfenidone-treated mice received pirfenidone (200 mg kg^{-1}) by oral gavage twice daily from days 18–24. Mice treated with compound **4** received 50 μL intratracheally, commencing on day 18 every 48 h for a total of four administrations. Control mice received vehicle (DMSO, 2%). Mice were culled on day 26. The lungs were perfused (via the right ventricle) with saline (5 mL) and the lungs lavaged with PBS (3 × 0.8 mL) containing EDTA (1 mM). BAL cells were combined and pelleted, and lavage fluid from the first lavage was snap-frozen. The lungs were removed, and the entire left lobe was removed and stored at −80 °C for analysis of total collagen. Two upper right lobes were removed, snap-frozen and stored at −80 °C for subsequent RNA analysis. The remaining lung was inflated with formalin (10%) and fixed for 24 h prior to removal into ethanol (70%) before being embedded in paraffin wax for histological examination.

Total lung collagen: Frozen left lobes were thawed, weighed, minced finely with scissors, and placed in pepsin (3 mg mL^{-1}, 5 mL) in acetic acid (0.5 M). Samples were incubated for 24 h at 4 °C, and cleared extract (0.2 mL) was incubated with Sircol reagent (Biocolor, 0.8 mL) for 60 min at room temperature. Collagen was sedimented by centrifugation at 10000 *g* for 5 min, and the pellets were resuspended in NaOH (0.5 M, 0.5 mL). Samples were examined for absorbance at 560 nm with reference to a collagen standard curve.

Estimation of vascular leakage: Vascular leakage was determined by measuring total protein in the lavage fluid by BCA assay (Pierce) with bovine serum albumin as standard.

Histological lung inflammation and fibrosis score: Fibrosis and histological score was carried out in stained (Masson's trichrome) sections. Inflammation (peribronchiolar, perivascular, and alveolar wall thickness) was scored in >5 random fields at magnification X630 with use of the following system: peribronchiolar and perivascular, 1 = no cells, 2 = <20 cells, 3 = 20–100 cells, 4 = >100 cells; alveolar wall thickness, 1 = no cells, 2 = 2–3 cells thick, 3 = 4–5 cells thick, 4 = >5 cells thick. The combined inflammatory score is the sum of these scores. Fibrosis score was evaluated as the area of the section positively stained for collagen (1 = none, 2 = <10%, 3 = <50%, 4 = >50%). Only fields in which the majority of the field was composed of alveoli were scored.

Determination of galectin-3 levels in BAL and serum by ELISA: Samples of BAL fluid and serum were assayed for galectin-3 and MCP-1 levels by ELISA (R&D systems).

Acknowledgements

This work was supported by grants to U.J.N. and H L. from the Swedish Research Council (Grants no. 621–2003–4265, 621–2006–3985, and 621–2009–5326), the programs "Glycoconjugates in Biological Systems" and "Chemistry for Life Sciences" sponsored by the Swedish Strategic Research Foundation, the foundation "Olle Engkvist Byggmästare", the Royal Physiographic Society, Lund, by the European Community's Seventh Framework Program (FP7–2007–2013) under grant agreement no. HEALTH-F2–2011–256986-project acronym PANACREAS, and a project grant awarded by the Knut and Alice Wallenberg Foundation (KAW 2013.0022). The in vivo experiments were supported by Galecto Biotech AB, Sweden. H.B. gratefully acknowledges the financial support from the Cancer Council Queensland, Australia (grants: ID1043716 and ID1080845). R.J.P. gratefully acknowledges the financial support from the Dutch Technology Foundation STW, applied science division of NOW. Barbro Kahl-Knutsson is acknowledged for performing fluorescence anisotropy experiments.

Keywords: antagonists · fibrosis · galectins · inhibitors · thiodigalactosides · vesicles

[1] P. Lajoie, J. G. Goetz, J. W. Dennis, I. R. Nabi, *J. Cell Biol.* **2009**, *185*, 381–385.
[2] C. Boscher, J. W. Dennis, I. R. Nabi, *Curr. Opin. Cell Biol.* **2011**, *23*, 383–392.
[3] F. T. Liu, G. A. Rabinovich, *Ann. N. Y. Acad. Sci.* **2010**, *1183*, 158–182.
[4] F.-T. Liu, G. A. Rabinovich, *Nat. Rev. Cancer* **2005**, *5*, 29–41.
[5] a) C.-I. Lin, E. E. Whang, D. B. Donner, X. Jiang, B. D. Price, A. M. Carothers, T. Delaine, H. Leffler, U. J. Nilsson, V. Nose, F. D. Moore, D. T. Ruan, *Mol. Cancer Res.* **2009**, *7*, 1655–1662; b) A. C. MacKinnon, S. L. Farnworth, P. S. Hodkinson, N. C. Henderson, K. M. Atkinson, H. Leffler, U. J. Nilsson, C. Haslett, S. J. Forbes, T. Sethi, *J. Immunol.* **2008**, *180*, 2650–2658.

[6] a) V. V. Glinsky, G. Kiriakova, O. V. Glinskii, V. V. Mossine, T. P. Mawhinney, J. R. Turk, A. B. Glinskii, V. H. Huxley, J. E. Price, G. V. Glinsky, *Neoplasia* **2009**, *11*, 901 – 909; b) A. C. Mackinnon, M. A. Gibbons, S. L. Farnworth, H. Leffler, U. J. Nilsson, T. Delaine, A. J. Simpson, S. J. Forbes, N. Hirani, J. Gauldie, T. Sethi, *Am. J. Respir. Crit. Care Med.* **2012**, *185*, 537 – 546.

[7] a) B. A. Salameh, H. Leffler, U. J. Nilsson, *Bioorg. Med. Chem. Lett.* **2005**, *15*, 3344 – 3346; b) B. A. Salameh, A. Sundin, H. Leffler, U. J. Nilsson, *Bioorg. Med. Chem.* **2006**, *14*, 1215 – 1220; c) P. Sörme, P. Arnoux, B. Kahl-Knutsson, H. Leffler, J. M. Rini, U. J. Nilsson, *J. Am. Chem. Soc.* **2005**, *127*, 1737 – 1743; d) P. Sörme, Y. Qian, P.-G. Nyholm, H. Leffler, U. J. Nilsson, *ChemBioChem* **2002**, *3*, 183 – 189; e) J. Tejler, B. Salameh, H. Leffler, U. J. Nilsson, *Org. Biomol. Chem.* **2009**, *7*, 3982 – 3990; f) S. Fort, H. S. Kim, O. Hindsgaul, *J. Org. Chem.* **2006**, *71*, 7146 – 7154; g) D. Giguère, S. André, M.-A. Bonin, M.-A. Bellefleur, A. Provencal, P. Cloutier, B. Pucci, R. Roy, H.-J. Gabius, *Bioorg. Med. Chem.* **2011**, *19*, 3280 – 3287; h) D. Giguère, M. Bonin, P. Cloutier, R. Patnam, C. Stpierre, S. Sato, R. Roy, *Bioorg. Med. Chem.* **2008**, *16*, 7811 – 7823; i) D. Giguère, R. Patnam, M.-A. Bellefleur, C. St. -Pierre, S. Sato, R. Roy, *Chem. Commun.* **2006**, 2379 – 2381; j) D. Giguère, S. Sato, C. St-Pierre, S. Sirois, R. Roy, *Bioorg. Med. Chem. Lett.* **2006**, *16*, 1668 – 1672; k) M. F. Marchiori, D. E. P. Souto, L. O. Bortot, J. F. Pereira, L. T. Kubota, R. D. Cummings, M. Dias-Baruffi, I. Carvalho, V. L. Campo, *Bioorg. Med. Chem.* **2015**, *23*, 3414 – 3425; l) G. A. Rabinovich, A. Cumashi, G. A. Bianco, D. Ciavardelli, I. Iurisci, M. D'Egidio, E. Piccolo, N. Tinari, N. Nifantiev, S. Iacobelli, *Glycobiology* **2005**, *16*, 210 – 220; m) S. R. Rauthu, T. C. Shiao, S. André, M. C. Miller, É. Madej, K. H. Mayo, H.-J. Gabius, R. Roy, *ChemBioChem* **2015**, *16*, 126 – 139.

[8] a) I. Cumpstey, E. Salomonsson, A. Sundin, H. Leffler, U. J. Nilsson, *Chem. Eur. J.* **2008**, *14*, 4233 – 4245; b) I. Cumpstey, A. Sundin, H. Leffler, U. J. Nilsson, *Angew. Chem. Int. Ed.* **2005**, *44*, 5110 – 5112; *Angew. Chem.* **2005**, *117*, 5240 – 5242; c) T. Delaine, I. Cumpstey, L. Ingrassia, M. Le Mercier, P. Okechukwu, H. Leffler, R. Kiss, U. J. Nilsson, *J. Med. Chem.* **2008**, *51*, 8109 – 8114; d) B. A. Salameh, I. Cumpstey, A. Sundin, H. Leffler, U. J. Nilsson, *Bioorg. Med. Chem.* **2010**, *18*, 5367 – 5378.

[9] M. Van Scherpenzeel, E. E. Moret, L. Ballell, R. M. J. Liskamp, U. J. Nilsson, H. Leffler, R. J. Pieters, *ChemBioChem* **2009**, *10*, 1724 – 1733.

[10] H. van Hattum, H. M. Branderhorst, E. E. Moret, U. J. Nilsson, H. Leffler, R. J. Pieters, *J. Med. Chem.* **2013**, *56*, 1350 – 1354.

[11] T. L. Lowary, O. Hindsgaul, *Carbohydr. Res.* **1994**, *251*, 33 – 67.

[12] a) P. Sörme, B. Kahl-Knutsson, M. Huflejt, U. J. Nilsson, H. Leffler, *Anal. Biochem.* **2004**, *334*, 36 – 47; b) P. Sörme, B. Kahl-Knutsson, U. Wellmar, U. J. Nilsson, H. Leffler, *Methods Enzymol.* **2003**, *362*, 504 – 512.

[13] a) S. Carlsson, M. C. Carlsson, H. Leffler, *Glycobiology* **2007**, *17*, 906 – 912; b) S. Carlsson, C. T. Öberg, M. C. Carlsson, A. Sundin, U. J. Nilsson, D. Smith, R. D. Cummings, J. Almkvist, A. Karlsson, H. Leffler, *Glycobiology* **2007**, *17*, 663 – 676.

[14] K. Bum-Erdene, I. A. Gagarinov, P. M. Collins, M. Winger, A. G. Pearson, J. C. Wilson, H. Leffler, U. J. Nilsson, I. D. Grice, H. Blanchard, *ChemBioChem* **2013**, *14*, 1331 – 1342.

[15] I. Cumpstey, E. Salomonsson, A. Sundin, H. Leffler, U. J. Nilsson, *ChemBioChem* **2007**, *8*, 1389 – 1398.

[16] a) K. Müller, C. Faeh, F. Diederich, *Science* **2007**, *317*, 1881 – 1886; b) R. Paulini, K. Müller, F. Diederich, *Angew. Chem. Int. Ed.* **2005**, *44*, 1788 – 1805; *Angew. Chem.* **2005**, *117*, 1820 – 1839; c) M. Zürcher, F. Diederich, *J. Org. Chem.* **2008**, *73*, 4345 – 4361.

[17] P. Zhou, J. Zou, F. Tian, Z. Shang, *J. Chem. Inf. Mod.* **2009**, *49*, 2344 – 2355.

[18] J. C. Biffinger, H. W. Kim, S. G. DiMagno, *ChemBioChem* **2004**, *5*, 622 – 627.

[19] D. N. Cooper, *Biochim Biophys Acta* **2002**, *1572*, 209 – 231.

[20] a) S. Aits, J. Kricker, B. Liu, A.-M. Ellegaard, S. Hämälistö, S. Tvingsholm, E. Corcelle-Termeau, S. Høgh, T. Farkas, A. Holm Jonassen, I. Gromova, M. Mortensen, M. Jäättelä, *Autophagy* **2015**, *11*, 1408 – 1424; b) I. Paz, M. Sachse, N. Dupont, J. Mounier, C. Cederfur, J. Enninga, H. Leffler, F. Poirier, M. C. Prevost, F. Lafont, P. Sansonetti, *Cell. Microbiol.* **2010**, *12*, 530 – 544.

[21] T. L. Thurston, M. P. Wandel, N. von Muhlinen, A. Foeglein, F. Randow, *Nature* **2012**, *482*, 414 – 418.

[22] N. H. Petersen, O. D. Olsen, L. Groth-Pedersen, A. M. Ellegaard, M. Bilgin, S. Redmer, M. S. Ostenfeld, D. Ulanet, T. H. Dovmark, A. Lonborg, S. D. Vindelov, D. Hanahan, C. Arenz, C. S. Ejsing, T. Kirkegaard, M. Rohde, J. Nylandsted, M. Jaattela, *Cancer Cell* **2013**, *24*, 379 – 393.

[23] V. Sarafian, M. Jadot, J. M. Foidart, J. J. Letesson, F. van den Brûle, V. Castronovo, R. Wattiaux, S. Wattiaux-De Coninck, *Int. J. Cancer* **1998**, *75*, 105 – 111.

[24] E. Salomonsson, A. Larumbe, J. Tejler, E. Tullberg, H. Rydberg, A. Sundin, T. Khabut, T. Frejd, Y. D. Lobsanov, J. M. Rini, U. J. Nilsson, H. Leffler, *Biochemistry* **2010**, *49*, 9518 – 9532.

[25] M. A. Gitt, S. M. Massa, H. Leffler, S. H. Barondes, *J. Biol. Chem.* **1992**, *267*, 10601 – 10606.

[26] S. M. Massa, D. N. Cooper, H. Leffler, S. H. Barondes, *Biochemistry* **1993**, *32*, 260 – 267.

[27] T. Magnaldo, D. Fowlis, M. Darmon, *Differentiation* **1998**, *63*, 159 – 168.

[28] I. Cumpstey, S. Carlsson, H. Leffler, U. J. Nilsson, *Org. Biomol. Chem.* **2005**, *3*, 1922 – 1932.

[29] C. T. Öberg, S. Carlsson, E. Fillion, H. Leffler, U. J. Nilsson, *Bioconjugate Chem.* **2003**, *14*, 1289 – 1297.

[30] P. M. Collins, K. I. P. J. Hidari, H. Blanchard, *Acta Crystallogr. Sect. D Biol. Crystallogr.* **2007**, *63*, 415 – 419.

[31] P. Evans, *Acta Crystallogr. Sect. D Biol. Crystallogr.* **2006**, *62*, 72 – 82.

[32] M. D. Winn, C. C. Ballard, K. D. Cowtan, E. J. Dodson, P. Emsley, P. R. Evans, R. M. Keegan, E. B. Krissinel, A. G. Leslie, A. McCoy, S. J. McNicholas, G. N. Murshudov, N. S. Pannu, E. A. Potterton, H. R. Powell, R. J. Read, A. Vagin, K. S. Wilson, *Acta Crystallogr. Sect. D Biol. Crystallogr.* **2011**, *67*, 235 – 242.

[33] J. Seetharaman, A. Kanigsberg, R. Slaaby, H. Leffler, S. H. Barondes, J. M. Rini, *J. Biol. Chem.* **1998**, *273*, 13047 – 13052.

[34] G. N. Murshudov, P. Skubak, A. A. Lebedev, N. S. Pannu, R. A. Steiner, R. A. Nicholls, M. D. Winn, F. Long, A. A. Vagin, *Acta Crystallogr. Sect. D Biol. Crystallogr.* **2011**, *67*, 355 – 367.

[35] R. J. Read, A. J. McCoy, *Acta Crystallogr. Sect. D Biol. Crystallogr.* **2011**, *67*, 338 – 344.

[36] P. Emsley, B. Lohkamp, W. G. Scott, K. Cowtan, *Acta Crystallogr. Sect. D Biol. Crystallogr.* **2010**, *66*, 486 – 501.

[37] A. W. Schüttelkopf, D. M. van Aalten, *Acta Crystallogr. Sect. D Biol. Crystallogr.* **2004**, *60*, 1355 – 1363.

[38] V. B. Chen, W. B. Arendall III, J. J. Headd, D. A. Keedy, R. M. Immormino, G. J. Kapral, L. W. Murray, J. S. Richardson, D. C. Richardson, *Acta Crystallogr. Sect. D Biol. Crystallogr.* **2010**, *66*, 12 – 21.

[39] S. McNicholas, E. Potterton, K. S. Wilson, M. E. Noble, *Acta Crystallogr. Sect. D Biol. Crystallogr.* **2011**, *67*, 386 – 394.

[40] E. Salomonsson, M. Carlsson, V. Osla, R. Hendus-Altenburger, B. Kahl Knutson, C. Oberg, A. Sundin, R. Nilsson, E. Nordberg-Karlsson, U. Nilsson, A. Karlsson, J. M. Rini, H. Leffler, *J. Biol. Chem.* **2010**, *285*, 35079 – 35091.

[41] M. K. Ho, T. A. Springer, *J. Immunol.* **1982**, *128*, 1221 – 1228.

Manuscript received: May 16, 2016

Accepted article published: June 29, 2016

Final article published: August 12, 2016